nature genetics

GRM1 is upregulated through gene fusion and promoter swapping in chondromyxoid fibroma

Karolin H Nord[1], Henrik Lilljebjörn[1], Francesco Vezzi[2], Jenny Nilsson[1], Linda Magnusson[1], Johnbosco Tayebwa[1], Danielle de Jong[3], Judith V M G Bovée[4], Pancras C W Hogendoorn[4] & Karoly Szuhai[3]

Glutamate receptors are well-known actors in the central and peripheral nervous systems, and altered glutamate signaling is implicated in several neurological and psychiatric disorders. It is increasingly recognized that such receptors may also have a role in tumor growth. Here we provide direct evidence of aberrant glutamate signaling in the development of a locally aggressive bone tumor, chondromyxoid fibroma (CMF). We subjected a series of CMFs to whole-genome mate-pair sequencing and RNA sequencing and found that the glutamate receptor gene *GRM1* recombines with several partner genes through promoter swapping and gene fusion events. The *GRM1* coding region remains intact, and 18 of 20 CMFs (90%) showed a more than 100-fold and up to 1,400-fold increase in *GRM1* expression levels compared to control tissues. Our findings unequivocally demonstrate that direct targeting of *GRM1* is a necessary and highly specific driver event for CMF development.

CMF is a cartilaginous bone tumor with morphological features that resemble different steps of chondrogenesis—spindle-shaped and stellate cells are embedded in a myxoid matrix that ranges from fibrous to cartilaginous[1,2]. The disease primarily affects young adults, and it is most commonly detected in the second and third decades of life. Treatment involves surgery alone, and prognosis is excellent, even after disease recurrence. However, the histopathological and clinical features of CMF may resemble those of other benign or even high-grade malignant cartilaginous tumors. A specific genetic biomarker for the diagnosis of CMF would therefore be of benefit but has hitherto been lacking.

Previous studies of CMF cytogenetics and genomics have shown recurrent rearrangements of various segments in chromosome 6 (6p23-25, 6q12-15 and 6q23-27), although no target gene has conclusively been identified in these regions, despite vigorous attempts by different groups (Mitelman database; see URLs)[3]. In the present study, all eight CMFs with aberrant karyotypes had structural rearrangements of chromosome 6 (**Supplementary Table 1**). To further delineate the structural rearrangements of chromosome 6 and their consequences, we analyzed six CMFs using SNP arrays (**Fig. 1a** and **Supplementary Table 2**). We also analyzed four of these CMFs by whole-genome mate-pair sequencing, and two of these four cases, as well as two additional CMFs, were also analyzed by RNA sequencing (**Table 1**). Chromosome 6 was affected by copy number aberrations in five of the six CMFs analyzed by SNP array (**Fig. 1a** and **Supplementary Table 2**). In fact, the only recurrent copy number imbalances in these six cases were losses affecting chromosome 6. Notably, two CMFs had deletions at 6q24 with a distal breakpoint between consecutive probe-binding sites at base-pair positions 146,278,959 and 146,304,603, located immediately upstream of the *GRM1* gene (**Fig. 1a**). In accordance with these findings, whole-genome mate-pair sequencing identified structural genomic rearrangements of the region surrounding *GRM1* in all four cases analyzed (**Fig. 1b** and **Supplementary Table 3**). We confirmed that these rearrangements fused the complete coding region of *GRM1* to regulatory segments from three different partner genes (**Fig. 1b**, **Table 1**, **Supplementary Fig. 1** and **Supplementary Table 3**). In two CMFs, mate-pair sequencing indicated juxtaposition of the *GRM1* and *COL12A1* genes, predicting altered *GRM1* expression under the influence of the *COL12A1* promoter. *COL12A1* is normally located at 6q13, and this band was rearranged in both cases, as determined by cytogenetic analysis. Furthermore, recurrent rearrangements of *COL12A1* have previously been reported in CMF[3,4], and this gene is also known to exchange regulatory sequences with *IRS4* and to increase its expressed levels in another benign bone- and cartilage-forming tumor known as subungual exostosis[5]. Mate-pair sequencing of another CMF showed juxtaposition of *GRM1* and the *TBL1XR1* gene at 3q26. The orientation of the sequence reads indicated that there was an inversion associated with the rearrangement, and SNP array data in this case identified a deletion immediately upstream of *GRM1*. The 5′ part of *TBL1XR1* could therefore have been inserted upstream of *GRM1*, which would place the expression of *GRM1* under the control of the *TBL1XR1* promoter. Interestingly, *TBL1XR1* has previously been shown to be fused to *TP63* in diffuse large B cell lymphoma[6]. In the remaining case, DNA mate-pair sequencing identified an inversion involving parts of chromosome arm 6q that would result in altered *GRM1* expression under the influence of the *BCLAF1* promoter. We confirmed the synthesis of a *BCLAF1-GRM1*

[1]Department of Clinical Genetics, University and Regional Laboratories, Skåne University Hospital, Lund University, Lund, Sweden. [2]Science for Life Laboratory, Department of Biochemistry and Biophysics, Stockholm University, Solna, Sweden. [3]Department of Molecular Cell Biology, Leiden University Medical Center, Leiden, The Netherlands. [4]Department of Pathology, Leiden University Medical Center, Leiden, The Netherlands. Correspondence should be addressed to K.H.N. (karolin.hansen_nord@med.lu.se).

Received 10 December 2013; accepted 27 February 2014; published online 23 March 2014; doi:10.1038/ng.2927

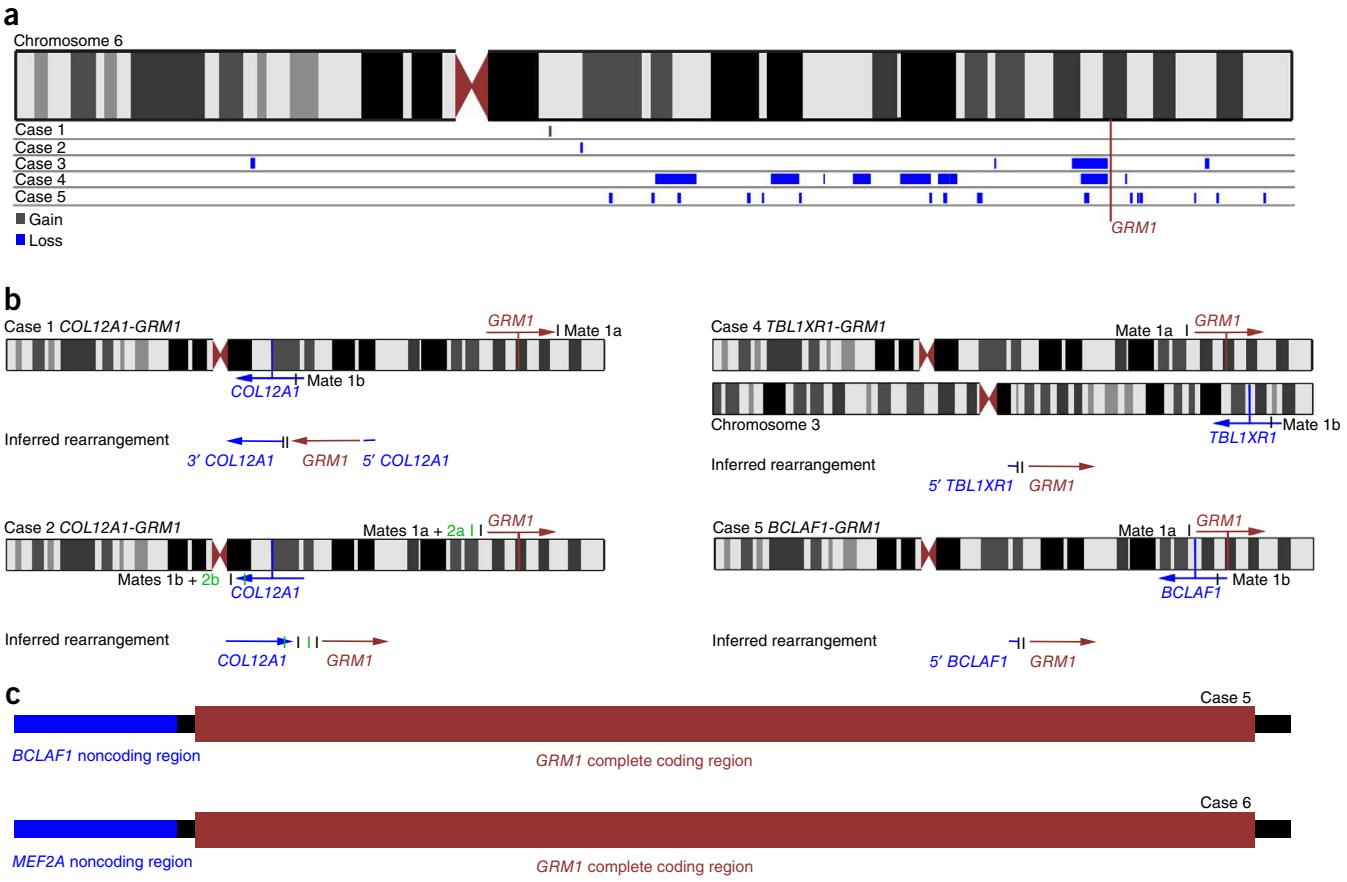

Figure 1 Rearrangements of chromosome 6 target the *GRM1* gene. (**a**) Genomic copy number alterations affecting chromosome 6 were detected in five CMFs by SNP array analysis. The most common aberrations were deletions at 6q24, and two of these deletions shared a common distal breakpoint immediately upstream of the *GRM1* gene. (**b**) In line with this finding, putative promoter swapping and gene fusion events that affected *GRM1* were found in all four CMFs analyzed by whole-genome mate-pair sequencing. Vertical lines represent the positions of mate-pair reads. (**c**) The *BCLAF1-GRM1* chimera detected in case 5 was confirmed by RNA sequencing, and this analysis also identified a *MEF2A-GRM1* fusion in case 6. In both fusions, the complete coding region of *GRM1* was intact, and upstream regulatory sequences were replaced by promoter swapping.

fusion transcript using RNA sequencing; this analysis also identified a *MEF2A-GRM1* fusion in an additional CMF (**Fig. 1c** and **Table 1**). We could validate both of these fusion transcripts by RT-PCR. In both cases, exon 1 of the 5′ partner gene (*BCLAF1* nucleotide 139, NM_014739 and *MEF2A* nucleotide 177, NM_001171894) was fused to exon 1 of *GRM1* (nucleotide 3, ENST00000392299). Neither *BCLAF1* nor *MEF2A* contributed any coding sequence to the resulting fusion gene. Instead, the regulatory sequences upstream of *GRM1* were replaced by the corresponding sequences of the partner genes. *BCLAF1* is located at 6q23 and, as with *COL12A1*, has previously been found to be rearranged in a number of CMFs[3]. *MEF2A* is located on chromosome 15 and lacks any previous connection with CMF, although it has been implicated in bone formation[7]. We screened an additional 19 CMFs for these fusions by RT-PCR and identified a *BCLAF1-GRM1* fusion in one additional case (**Table 1**). It is not surprising that a hybrid *GRM1* transcript was not confirmed in all cases—as exemplified by cases 2 and 7, promoter swapping does not always lead to the expression of a chimeric transcript (**Table 1**). Also, there are most likely more 5′ partner genes for *GRM1* than have currently been detected, and fusion genes involving such previously unidentified partners would not have been identified with the present RT-PCR primers. We corroborated genomic rearrangement of the *GRM1* promoter region by FISH analysis in five cases, two of which had shown evidence of promoter swapping in whole-genome mate-pair sequencing (**Table 1** and **Supplementary Fig. 2**).

In summary, *GRM1* recombines with several different 5′ partner genes, which we predict will lead to upregulated expression of transcripts comprising the complete coding region of *GRM1* either with or without noncoding remnants of the 5′ partner gene. Hence, we postulate that the key pathogenetic event in CMF is upregulation of the entire *GRM1* gene. In support of this hypothesis, we found remarkably high gene expression levels for *GRM1* by real-time quantitative PCR (RT-qPCR) (**Fig. 2**). In 18 of the 20 CMFs analyzed, there was a more than 100-fold and up to 1,400-fold increase in *GRM1* expression levels compared to other cartilaginous tumors, all of which showed either very low or no expression of this gene. The results were the same regardless of which endogenous control gene was used. In our analysis of available global gene expression data for 174 non-CMF mesenchymal tumors (including 19 subtypes of chondrogenic bone tumors and adipocytic, fibroblastic/myofibroblastic and smooth-muscle soft-tissue tumors, as well as soft-tissue tumors of uncertain differentiation), only 1 case showed expression levels for *GRM1* that were clearly above the noise level of the array (**Supplementary Table 4a**). Thus, 90% of the present CMFs showed highly elevated expression levels for *GRM1*. This upregulation is due to genomic rearrangements that place *GRM1* under the influence of a strong promoter: in some cases, promoter swapping leads to high expression

Table 1 Clinical and molecular genetic data on CMF

Case	Age (years)	Sex	Tumor location	Cytogenetic and SNP array analyses[a]	*GRM1* promoter swapping[b]	*GRM1* transcript[c]	*GRM1* expression levels[d]
1	29	M	Tibia	Chr. 6 aberrant	*COL12A1*	NA	NA
2	14	M	Tibia	Chr. 6 aberrant	*COL12A1*, split FISH signals	Intact *GRM1*	High
3	57	M	Os ischium	Chr. 6 aberrant	Deletion 5′ of *GRM1*	RT-PCR negative	High
4	39	M	Sternum	Chr. 6 aberrant	*TBL1XR1*, deletion 5′ of *GRM1*, FISH negative	RT-PCR negative[e]	NA[e]
5	34	F	Os ilium	Chr. 6 aberrant	*BCLAF1*, split FISH signals	*BCLAF1-GRM1*	High
6	12	F	Foot	Chr. 6 aberrant	NA	*MEF2A-GRM1*	High
7	71	F	Tibia	Chr. 6 aberrant	Split FISH signals	Intact *GRM1*	High
8	46	M	Tibia	46, XY	Split FISH signals	*BCLAF1-GRM1*	High
9	17	M	Femur	46, XY	NA	RT-PCR negative	High
10	22	M	Tibia	46, XY	NA	RT-PCR negative	High
11	4	M	Tibia	Chr. 6 aberrant	NA	RT-PCR negative	High
12	13	M	Tibia	Chr. 6 aberrant	NA	RT-PCR negative	High
13	18	F	Tibia	46, XX	NA	RT-PCR negative	Low
14	63	M	Tibia	NA	NA	RT-PCR negative	High
15	19	M	Foot	NA	NA	RT-PCR negative	High
16	15	M	Foot	NA	NA	RT-PCR negative	High
17	12	F	Hand	NA	Split FISH signals	RT-PCR negative	High
18	15	F	Tibia	NA	FISH negative	RT-PCR negative	High
19	13	M	Tibia	Chr. 6 aberrant	FISH negative	RT-PCR negative	High
20	10	F	Foot	NA	FISH negative	RT-PCR negative	Low
21	42	M	Rib	NA	FISH negative	RT-PCR negative	High
22	25	M	Femur	NA	NA	RT-PCR negative	High

NA, not analyzed; M, male; F, female.
[a]Chr. 6 aberrant, cytogenetic and/or SNP array analyses identified aberrations affecting chromosome 6. [b]The *GRM1* mate-pair partner gene identified through DNA mate-pair sequencing is indicated. Genomic rearrangement of the *GRM1* promoter region was also detected by SNP array and FISH analyses. [c]Intact *GRM1*, high expression of an intact *GRM1* transcript was identified using RNA sequencing analysis; RT-PCR negative, RT-PCR analyses for the *BCLAF1-GRM1* and *MEF2A-GRM1* fusion transcripts were negative. [d]*GRM1* expression levels evaluated by RT-qPCR. [e]No *TBL1XR1-GRM1* fusion transcript was found by RT-PCR in case 4. The amount of RNA was not sufficient for RT-qPCR in this case.

of a hybrid gene, and in others swapping leads to increased expression of an intact *GRM1* transcript (**Table 1** and **Supplementary Table 4b**). These findings were corroborated using SNP array, whole-genome mate-pair sequencing, RNA sequencing, RT-PCR and FISH analyses and are consistent with the fact that chromosomal rearrangement of 6q24, where *GRM1* is located, is a cytogenetic hallmark of CMF (Mitelman database; see URLs). In 10% of the present CMFs, we did not find upregulation of *GRM1* expression, which may suggest that a small subset of CMFs develops through a different genetic route than *GRM1* activation.

Glutamate receptor metabotropic 1 (GRM1) is one of eight metabotropic glutamate receptors, denoted GRM1–GRM8, all of which are G protein–coupled receptors. These receptors can be subdivided into three groups on the basis of sequence homology and the second messenger systems that they activate. Group I receptors, including GRM1, activate phospholipase C and downstream signaling pathways such as protein kinase C (PKC), calcium ion, PIK3CA-AKT1-MTOR and mitogen-activated protein kinase (MAPK) signaling[8]. Unfortunately, the lack of CMF cell lines prohibits further evaluation of the functional consequences of *GRM1* overexpression *in vitro*. This problem is common to most mesenchymal tumors, reflecting the fact that it is exceedingly difficult to establish stable cell lines from such tumors. Therefore, we attempted to determine whether aberrant *GRM1* expression in CMF leads to abnormal activation of downstream signaling pathways by studying the expression of the GRM1 target genes *AKT2*, *MAPK1* and *BCL2* in CMF using our RNA sequencing data (**Supplementary Table 4b**). We indeed confirmed expression of these genes in CMF, although differences in their expression levels could not be attributed to *GRM1* overexpression. AKT2, MAPK1 and BCL2 are downstream effectors in many signaling pathways known to be involved in tumor formation and are therefore not specific for GRM1 activation. Nonetheless, hyperactive GRM1 signaling in CMF is strongly supported by the present genetic findings and agrees well with the recently reported role of glutamate receptors in tumor development. Aberrant expression of GRM1 has been associated with, for example, malignant melanoma and breast cancer[9,10], and it has been shown to transform epithelial cells[11]. Activation of other metabotropic glutamate receptors has been suggested in several tumor types, including malignant melanoma, glioma and colorectal carcinoma[12–15].

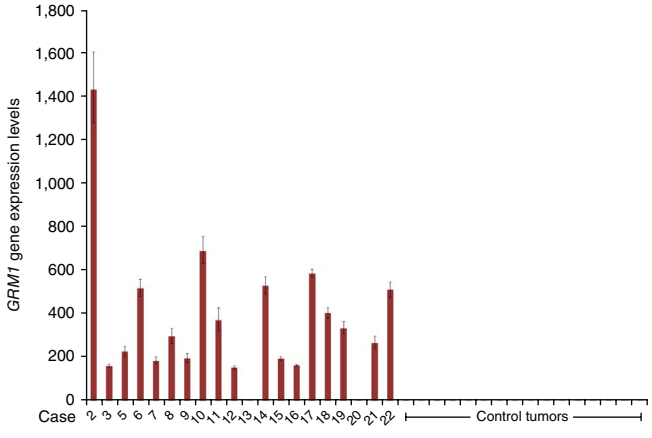

Figure 2 Rearrangements of chromosome 6 result in upregulation of the *GRM1* gene. Genomic rearrangements in CMF resulted in upregulation of the *GRM1* gene, as detected by RT-qPCR. The vast majority of CMFs (18/20) showed exceptionally high expression levels for this gene, whereas the control tissues showed either very low or no *GRM1* expression. The controls included three tumors each of extraskeletal myxoid chondrosarcoma, central conventional chondrosarcoma, chondroma and osteochondroma, as well as two synovial chondromatoses and two chondroblastic osteosarcomas, presented from left to right. Error bars represent the range of three technical replicates.

Furthermore, inhibition of glutamate signaling impairs growth, migration and invasion and induces apoptosis in melanoma, glioma, and breast and prostate cancer cells[8]. Pharmacological targeting of metabotropic glutamate receptors has therefore been suggested as a potential treatment strategy for these diseases. Somatic mutations in *GRM1* have been found in a wide variety of cancers, and it is interesting to note that most of these previously detected mutations are missense variants, suggesting that activation rather than truncation of the encoded protein is beneficial for transformation[8]. As CMF is a mesenchymal bone tumor, it should also be noted that *GRM4* was recently found to contain a susceptibility locus for osteosarcoma, the most common primary bone tumor of adolescents and young adults[16]. In line with this finding, the glutamate receptors *GRM4*, *GRM5* and *GRM6* are expressed in non-CMF chondrogenic and osteogenic bone tumors as well as in normal osteoblasts and osteoclasts[17] (**Supplementary Table 4c**), suggesting that these receptors are involved in the regulation of both normal and neoplastic bone formation. Chondrocytes have also been shown to express glutamate receptors[18,19], and normal human cartilage expresses *GRM1* and *GRM2* in addition to *GRM4*, *GRM5* and *GRM6* (**Supplementary Table 4c**). Furthermore, both bone and cartilage cells are able to release endogenous glutamate[20,21].

In conclusion, we show that metabotropic glutamate receptor 1 is activated through gene fusion and promoter swapping in a benign mesenchymal tumor. Neither this mechanism of activation nor the affected tumor type has previously been associated with glutamate receptor signaling. Upregulation of *GRM1* expression was remarkably prevalent in CMF, indicating that altered signaling through this receptor is likely crucial for tumor development. Further studies are needed to evaluate whether pharmacological targeting of *GRM1* signaling could constitute a supplementary treatment strategy for patients with CMF. We note that a drug that interferes with GRM1 signaling is already approved for clinical use[8]. The exceptionally specific upregulation of *GRM1* expression in CMF suggests that this biomarker could very soon be useful in the clinical discrimination of CMF from its mimics.

URLs. Database of Genomic Variants, http://dgv.tcag.ca/; Integrative Genomics Viewer, http://www.broadinstitute.org/igv/; FindTranslocations tool, https://github.com/vezzi/FindTranslocations; Mitelman Database of Chromosome Aberrations and Gene Fusions in Cancer, http://cgap.nci.nih.gov/Chromosomes/Mitelman.

METHODS

Methods and any associated references are available in the online version of the paper.

Note: Any Supplementary Information and Source Data files are available in the online version of the paper.

ACKNOWLEDGMENTS

We are grateful for the expert technical assistance of M. Rissler. We acknowledge help with the microarray analyses from the Swegene Centre for Integrative Biology at Lund University, support from the Science for Life Laboratory, the National Genomics Infrastructure (NGI), Sweden, and the Knut and Alice Wallenberg Foundation, and UPPMAX for providing assistance with massively parallel DNA sequencing and computational infrastructure. This work was supported by the Magnus Bergvall Foundation, the Royal Physiographic Society (Lund, Sweden) and the Swedish Childhood Cancer Foundation.

AUTHOR CONTRIBUTIONS

K.H.N., H.L., J.V.M.G.B., P.C.W.H. and K.S. conceived and designed the experiments. J.N. and K.H.N. analyzed SNP array data. H.L., K.H.N. and J.T. carried out bioinformatic analyses of RNA sequencing data and global gene expression data. F.V. developed an algorithm for the analysis of DNA mate-pair sequencing data. F.V., K.S. and K.H.N. analyzed DNA mate-pair sequencing data and interpreted the results. J.N. and L.M. conducted RT-PCR and RT-qPCR experiments. L.M., D.d.J. and K.S. performed FISH analyses. K.H.N. prepared the manuscript with contributions from all other authors.

COMPETING FINANCIAL INTERESTS

The authors declare no competing financial interests.

1. Romeo, S. *et al.* Chondromyxoid fibroma resembles *in vitro* chondrogenesis, but differs in expression of signalling molecules. *J. Pathol.* **206**, 135–142 (2005).
2. Romeo, S., Aigner, T. & Bridge, J.A. in *WHO Classification of Tumours of Soft Tissue and Bone* (eds. Fletcher, C.D.M., Bridge, J.A., Hogendoorn, P.C.W. & Mertens, F.) 255–256 (IARC, Lyon, France, 2013).
3. Romeo, S. *et al.* Heterogeneous and complex rearrangements of chromosome arm 6q in chondromyxoid fibroma: delineation of breakpoints and analysis of candidate target genes. *Am. J. Pathol.* **177**, 1365–1376 (2010).
4. Yasuda, T. *et al.* Aberrations of 6q13 mapped to the *COL12A1* locus in chondromyxoid fibroma. *Mod. Pathol.* **22**, 1499–1506 (2009).
5. Mertens, F. *et al.* The t(X;6) in subungual exostosis results in transcriptional deregulation of the gene for insulin receptor substrate 4. *Int. J. Cancer* **128**, 487–491 (2011).
6. Scott, D.W. *et al. TBL1XR1/TP63*: a novel recurrent gene fusion in B-cell non-Hodgkin lymphoma. *Blood* **119**, 4949–4952 (2012).
7. Leupin, O. *et al.* Control of the *SOST* bone enhancer by PTH using MEF2 transcription factors. *J. Bone Miner. Res.* **22**, 1957–1967 (2007).
8. Willard, S.S. & Koochekpour, S. Glutamate signaling in benign and malignant disorders: current status, future perspectives, and therapeutic implications. *Int. J. Biol. Sci.* **9**, 728–742 (2013).
9. Mehta, M.S. *et al.* Metabotropic glutamate receptor 1 expression and its polymorphic variants associate with breast cancer phenotypes. *PLoS ONE* **8**, e69851 (2013).
10. Namkoong, J. *et al.* Metabotropic glutamate receptor 1 and glutamate signaling in human melanoma. *Cancer Res.* **67**, 2298–2305 (2007).
11. Martino, J.J. *et al.* Metabotropic glutamate receptor 1 (Grm1) is an oncogene in epithelial cells. *Oncogene* **32**, 4366–4376 (2013).
12. Prickett, T.D. *et al.* Exon capture analysis of G protein–coupled receptors identifies activating mutations in *GRM3* in melanoma. *Nat. Genet.* **43**, 1119–1126 (2011).
13. Choi, K.Y., Chang, K., Pickel, J.M., Badger, J.D. II & Roche, K.W. Expression of the metabotropic glutamate receptor 5 (mGluR5) induces melanoma in transgenic mice. *Proc. Natl. Acad. Sci. USA* **108**, 15219–15224 (2011).
14. Ciceroni, C. *et al.* Type-3 metabotropic glutamate receptors regulate chemoresistance in glioma stem cells, and their levels are inversely related to survival in patients with malignant gliomas. *Cell Death Differ.* **20**, 396–407 (2013).
15. Chang, H.J. *et al.* Metabotropic glutamate receptor 4 expression in colorectal carcinoma and its prognostic significance. *Clin. Cancer Res.* **11**, 3288–3295 (2005).
16. Savage, S.A. *et al.* Genome-wide association study identifies two susceptibility loci for osteosarcoma. *Nat. Genet.* **45**, 799–803 (2013).
17. Chenu, C., Serre, C.M., Raynal, C., Burt-Pichat, B. & Delmas, P.D. Glutamate receptors are expressed by bone cells and are involved in bone resorption. *Bone* **22**, 295–299 (1998).
18. Wang, L., Hinoi, E., Takemori, A., Takarada, T. & Yoneda, Y. Abolition of chondral mineralization by group III metabotropic glutamate receptors expressed in rodent cartilage. *Br. J. Pharmacol.* **146**, 732–743 (2005).
19. Wang, L., Hinoi, E., Takemori, A., Nakamichi, N. & Yoneda, Y. Glutamate inhibits chondral mineralization through apoptotic cell death mediated by retrograde operation of the cystine/glutamate antiporter. *J. Biol. Chem.* **281**, 24553–24565 (2006).
20. Wang, L., Hinoi, E., Takemori, A. & Yoneda, Y. Release of endogenous glutamate by AMPA receptors expressed in cultured rat costal chondrocytes. *Biol. Pharm. Bull.* **28**, 990–993 (2005).
21. Genever, P.G. & Skerry, T.M. Regulation of spontaneous glutamate release activity in osteoblastic cells and its role in differentiation and survival: evidence for intrinsic glutamatergic signaling in bone. *FASEB J.* **15**, 1586–1588 (2001).

ONLINE METHODS

Subject information and tumor material. Tumor material was available from 22 CMF cases, treated at the Leiden University Medical Center (Leiden, The Netherlands), the Skåne University Hospital (Lund, Sweden) and the Karolinska University Hospital (Stockholm, Sweden). The age of the subjects ranged from 4–71 years (median of 19 years), and the majority of cases (15/22) were male. Tumors were located in the tibia (11), foot (4), femur (2), hand (1), os ischium (1), os ilium (1), sternum (1) and rib (1). Detailed information for the cases can be found in **Table 1**.

Ethics statement. All samples were obtained after informed consent procedures according to local ethical rules. The study was approved by the Regional Ethics Committees of Lund University, and the study protocol followed the rules set by the ethical board of Leiden University Medical Center and Dutch national rules for the secondary use of human material for research purposes.

Cytogenetic analyses. Chromosome banding analyses were performed according to standard methods[22], and karyotypes were described according to the recommendations in *ISCN (2013): An International System for Human Cytogenetic Nomenclature*[23].

Genomic copy number and loss-of-heterozygosity analyses. SNP array analysis was used for combined DNA copy number and LOH investigation in cases 1–6. DNA was extracted according to standard procedures[24] and hybridized to Illumina Human Omni-Quad BeadChips, which contain more than 1 million reporters, following protocols supplied by the manufacturer. Data analysis was performed using GenomeStudio software (Illumina), detecting imbalances by visual inspection. SNP positions were based on the GRCh37/hg19 sequence assembly. Constitutional copy number variations were excluded through comparison with the Database of Genomic Variants[25].

Whole-genome mate-pair sequencing for the detection of structural aberrations. To detect structural chromosome aberrations, DNA was extracted as described[24], and mate-pair libraries from cases 1, 2, 4 and 5 were prepared for sequencing using the Nextera mate-pair sample preparation kit according to the manufacturer's instructions (Illumina). The average insert size was 2–3 kb. In brief, 1 µg of DNA was prepared using the gel-free mate-pair library protocol, and paired-end 100-bp reads were retrieved from an Illumina HiSeq instrument. Sequencing depth was on average 2.3× (mapping coverage of 1.2×), resulting in 23× spanning coverage of the human genome. All samples were sequenced with high quality and yield; between 35.8 and 38.5 million read pairs were obtained for each sample, and average quality scores were 34.9–35.2 (>90% of bases ≥ Q30). Alignment against the GRCh37/hg19 build was performed using the Burrows-Wheeler Aligner (BWA) v. 0.7.2 software package. To identify structural rearrangements, sequence data were analyzed using BamView and the Integrative Genomics Viewer[26], as well as a freely available custom tool denoted FindTranslocations. The source code for this tool is available via GitHub (see URLs). A description of this algorithm as well as the filters used can be found in **Supplementary Table 5**.

RNA sequencing for fusion gene detection and analysis of gene expression levels. RNA was extracted according to standard procedures[24], and mRNA libraries from cases 2, 5, 6 and 7 were prepared for sequencing using TruSeq RNA Sample Prep Kit v2 according to the manufacturer's protocol (Illumina). In brief, 200–1,000 ng of total RNA was enriched for polyadenylated RNA using magnetic oligo(dT) beads. Enriched RNA was fragmented to a median size of 400 nucleotides by thermal fragmentation at 94 °C for 10 s in Elute, Prime, Fragment buffer. Fragmented RNA was used as template for cDNA synthesis with SuperScript II reverse transcriptase (Life Technologies). A second DNA strand was synthesized using DNA polymerase I and RNase H. After end repair and 3′-end adenylation, indexed adaptors were ligated to the double-stranded cDNA fragments. Adaptor-bound fragments were then enriched using 15-cycle PCR. Paired-end 101-bp reads were generated from the cDNA libraries using a HiScanSQ instrument (Illumina).

To identify candidate fusion transcripts from the sequence data, analyses were performed on gzip-compressed fastq files using TopHat v2.0.7 with the –fusion-search and –bowtie1 options, only allowing for the detection of fusions within a minimum distance of 100,000 bp (–fusion-min-dist option). The GRCh37/hg19 build was used as the human genome reference. The mate inner distance (–r option) was set to 200 with s.d. (–mate-std-dev option) of 200. TopHat-fusion-post was run on the output files from TopHat v2.0.7 to filter for fusions with at least one fusion-spanning read and two fusion-spanning mate pairs[27].

Gene expression levels were estimated from the TopHat alignments as fragments per kilobase of transcript per million mapped reads (FPKM) using Cufflinks v2.1.1. *De novo* transcript discovery was not used. Expression levels were estimated for a list of known protein-coding transcripts, as annotated by UCSC in March 2012.

RT-PCR for *GRM1* gene fusions. RT-PCR for the detection of *GRM1* gene fusions was performed as described[28]. Primer sequences are available in **Supplementary Table 6**. Amplified fragments were purified from an agarose gel and directly sequenced using the BigDye v1.1 Cycle Sequencing kit on an ABI 3130 Genetic Analyzer (Applied Biosystems). BLASTN software was used for the analysis of sequence data.

Real-time quantitative PCR. The relative expression levels of *GRM1* (Hs00168250_m1) were investigated in 20 CMFs using RT-qPCR and TaqMan Gene Expression assays (Applied Biosystems). Included as control tissues were three tumors each of extraskeletal myxoid chondrosarcoma, central conventional chondrosarcoma, chondroma and osteochondroma, as well as two chondroblastic osteosarcomas and two synovial chondromatoses. The *TBP* (4333769-F), *ACTB* (4333762-T) and *HPRT1* (Hs02800695_m1) genes were used as endogenous controls. Calculations were performed using the comparative C_t method (i.e., $\Delta\Delta C_t$). All reactions were performed in triplicate and were assayed on a 7500 RT-PCR system (Applied Biosystems).

Global gene expression data on bone and soft-tissue tumors. Global gene expression data were available for chondrogenic bone tumors (including for osteochondroma, subungual exostosis and bizarre parosteal osteochondromatous proliferation) and adipocytic, fibroblastic/myofibroblastic and smooth-muscle soft-tissue tumors, as well as for soft-tissue tumors of uncertain differentiation (including extraskeletal myxoid chondrosarcoma and ossifying fibromyxoid tumor). These data had previously been obtained using Affymetrix Human Gene 1.0 ST arrays according to the manufacturer's instructions. Also, publicly available global gene expression data sets on bone tumor samples and cell lines as well as normal bone and cartilage tissues were downloaded from the Gene Expression Omnibus (accessions GSE35545, GSE12865, GSE39795, GSE32395 and GSE19357). Gene expression data were normalized, background corrected and summarized using the Robust Multichip Analysis algorithm implemented in Expression Console version 1.1 software (Affymetrix).

FISH analysis. Genomic rearrangements of sequences immediately upstream of *GRM1* were investigated using FISH analysis. In brief, BAC clones mapping to *GRM1* and upstream sequences (**Supplementary Fig. 2**) were labeled and hybridized to interphase chromosome preparations as previously described[29,30]. Signals from more than 50 interphase nuclei were counted for each tumor. Rearrangement of the *GRM1* promoter region was defined as split signals in more than 20% of the analyzed nuclei.

22. Mandahl, N. in *Human Cytogenetics: Malignancy and Acquired Abnormalities* (ed. Rooney, D.E.) 165–203 (Oxford University Press, New York, 2001).
23. Shaffer, L.G., McGowan-Jordan, J. & Schmid, M. *ISCN (2013): An International System for Human Cytogenetic Nomenclature* (S. Karger, Basel, Switzerland, 2013).
24. Nord, K.H. *et al.* Concomitant deletions of tumor suppressor genes *MEN1* and *AIP* are essential for the pathogenesis of the brown fat tumor hibernoma. *Proc. Natl. Acad. Sci. USA* **107**, 21122–21127 (2010).
25. Iafrate, A.J. *et al.* Detection of large-scale variation in the human genome. *Nat. Genet.* **36**, 949–951 (2004).
26. Carver, T. *et al.* BamView: visualizing and interpretation of next-generation sequencing read alignments. *Brief. Bioinform.* **14**, 203–212 (2013).
27. Kim, D. *et al.* TopHat2: accurate alignment of transcriptomes in the presence of insertions, deletions and gene fusions. *Genome Biol.* **14**, R36 (2013).
28. Mohajeri, A. *et al.* Comprehensive genetic analysis identifies a pathognomonic *NAB2/STAT6* fusion gene, nonrandom secondary genomic imbalances, and a characteristic gene expression profile in solitary fibrous tumor. *Genes Chromosom. Cancer* **52**, 873–886 (2013).
29. Jin, Y. *et al.* Fusion of the *AHRR* and *NCOA2* genes through a recurrent translocation t(5;8)(p15;q13) in soft tissue angiofibroma results in upregulation of aryl hydrocarbon receptor target genes. *Genes Chromosom. Cancer* **51**, 510–520 (2012).
30. Rossi, S. *et al. EWSR1-CREB1* and *EWSR1-ATF1* fusion genes in angiomatoid fibrous histiocytoma. *Clin. Cancer Res.* **13**, 7322–7328 (2007).

doi:10.1038/ng.2927